Characterizing the Performance of Haleakala as a Ground Site for Laser Communications

Billy D. Felton and Randall J. Alliss

Northrop Grumman Information Systems
7555 Colshire Dr
McLean, VA 22102

Abstract

Radio Frequency (RF) signals have been relied on exclusively and successfully to communicate with spacecraft since satellite communications began nearly 60 years ago. However, missions now demand higher data rates to meet their data collection requirements. In response to this need, several organizations have begun to take steps to increase the data capacity of future missions by developing laser communications terminals and operational concepts for future missions. For example, NASA's Lunar Laser Communications Demonstration (LLCD) successfully demonstrated high data rate communications links to and from the LADEE satellite orbiting the moon during the Fall of 2013. As a next step, the Laser Communication Relay Demonstration (LCRD) will build upon the experience gained from LLCD and perform multi-year testing of Free-Space Optical Communications (FSOC) from geosynchronous orbit. Planning for these missions has included identifying candidate ground station locations, quantifying the impacts of the atmosphere on the data links, and developing operational concepts for mitigating transmission losses due to clouds, turbulence, and aerosols.

Since space-to-ground optical communications are adversely affected by the presence of clouds, turbulence, and other atmospheric phenomena, it is important to study the effects of the atmosphere on the communications link. To support this, Northrop Grumman is leading a campaign to measure and model the atmospheric effects on the link between a ground station on the summit of Haleakala and a satellite in geostationary orbit. Part of this effort involves using a modified version of the Weather Research & Forecast (WRF) model to generate long-term climatologies of optical turbulence parameters as well as to characterize the atmosphere along line-of-sight (LOS) from the ground station to the satellite during operations to be used as a link diagnostic tool. While ground-based instruments can be used to measure the effects of turbulence integrated along the entire LOS, they cannot generally be used to identify the vertical structure of turbulence. In this work, WRF is used to generate a three-dimensional representation of C_n^2 and other atmospheric parameters in both the planetary boundary layer and the free atmosphere. This allows for the characterization of C_n^2 along the entire portion of the LOS below 20-km above mean sea level along with estimates of the Fried Coherence length (r_0) and other seeing parameters along the LOS. In addition, a suite of ground-based sensors will be deployed, including a meteorological station, a whole-sky imager, and a ceilometer. Their measurements will be combined with output from WRF to support mission planning and the development of operational concepts for mitigating link outages. In particular, the *in situ* cloud data will be used along with multispectral geostationary satellite imagery and WRF model soundings to characterize and predict cloud heights and cloud encroachment over the summit of Haleakala. For this work, the WRF model is configured to run at 1-km horizontal resolution over a domain that includes the major observatories on the Big Island of Hawaii as well as Haleakala on Maui. Results from this work will be used to quantify the effects of the atmosphere on FSOC communications, diagnose link disruptions, and to develop atmospheric mitigation strategies.

1. Introduction

With ever-increasing amounts of data being generated, collected, and transmitted by the general public, scientists, and the military, modern society is increasingly reliant on high-performance satellite communications. As users continue to demand more data, the existing communications infrastructure will have to expand to meet the demands. Radio Frequency (RF) signals have been relied on exclusively and successfully to communicate with spacecraft since satellite communications began nearly 60 years ago, but there are limitations that may prevent RF communications from fully meeting future requirements. These technological, regulatory, and financial limitations may be alleviated, in part, by Free-Space Optical Communications (FSOC) systems. There are several key advantages to using FSOC to meet future communications requirements. Data can be transmitted through free-space via lasers at very high data rates of multi-Gb/s over long distances. Optical beams are very narrow, and are much less susceptible to interference or interception than RF signals. Unlike RF, the optical spectrum is unregulated. Finally, optical communications systems are relatively small and potentially much less expensive than comparable RF systems, particularly for space missions.

The ultimate realization of practical, high-availability FSOC systems, however, will depend upon how well they mitigate the impacts of atmospheric effects, primarily cloud cover and optical turbulence (OT). Clouds are the largest source of atmospheric attenuation for space-to-ground optical communications, often producing transmission losses of several decibels (dB) to several tens of dB. Without impractically large link margins, most clouds are generally considered blockages to FSOC links. Optical turbulence distorts light as it travels through the atmosphere, creating fluctuations in the power received by the ground station and distortions of the phase of the transmitted wave. Though usually not as significant a problem as clouds and turbulence, aerosols also attenuate optical signals and must be accounted for in a system's link budget. Finally, operations of FSOC systems can be affected by standard weather conditions; in particular, high winds, precipitation, and condensation may force closure of an open dome to protect sensitive optical equipment. Each of these atmospheric effects requires one or more different mitigation strategies, which may in turn be dependent on the operational design of a particular system.

Northrop Grumman is leading a campaign to measure and model the atmospheric effects on the link between a ground station on the summit of Haleakala and a satellite in geostationary orbit. Rising to 10,023 feet (3055 meters) above sea level, Haleakala is a massive volcano that makes up more than 75% of the Hawaiian Island of Maui. Its height, remoteness, and atmospheric characteristics make it a very desirable and sought-after location for ground-based telescopes such as the Mees Solar Observatory, the Advanced Electro-Optical System (AEOS), the Air Force Maui Optical Station (AMOS), and the Daniel K. Inouye Solar Telescope (DKIST) (Haleakala Observatories, 2015). Haleakala was selected for these telescopes, in part, because its summit benefits from a unique interaction of terrain and atmospheric circulations, with its peak often sitting above the cloud layer that frequently encircles its lower slopes.

Located nearly 4000 km from the nearest large land mass, the Hawaiian Islands experience a persistent "trade wind" flow, with winds in this tropical maritime environment usually blowing from the northeast or east. Forced by the Hadley cell circulation, the trade winds carry warm, moist air. Since cooling of the air with altitude leads to cloud formation, completely cloudless skies are rare in Hawaii. However, when the trade winds are blowing, the height of the moist surface air is usually limited by a strong temperature inversion that forms where descending cool air meets ascending warm air. The trade wind inversion can be identified in vertical profiles of atmospheric measurements by an increase in temperature and a sharp decrease in atmospheric moisture. A good example of this is shown in the Skew-T Log-P diagram in Figure 1 for Hilo, HI. The temperature profile (solid black line) increases with height between about 800 mb and 760 mb (~2000-2400 m AMSL) and the dew point temperature (dashed line) decreases sharply at the same level. When present, the temperature inversion limits the height to which

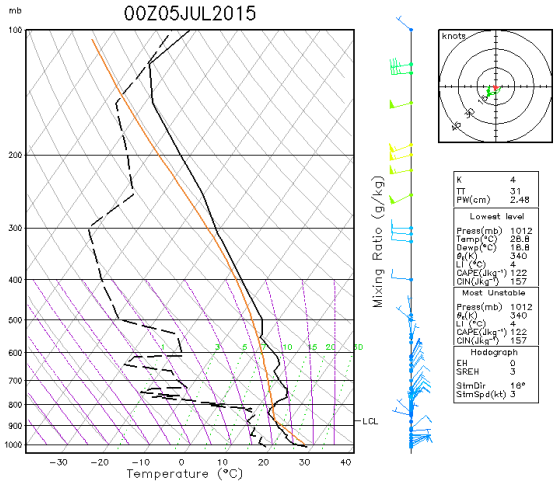

Figure 1 Hilo Skew-T Log-P diagram for 0000 UTC on July 5, 2015, with temperature (solid black line) and dew point temperature (dashed black line).

boundary layer clouds can grow. The height at which this temperature inversion exists varies, but usually occurs between 1500 and 2500 meters AMSL, meaning the summit of Haleakala is *usually* above the cloud tops. However, sometimes the inversion is higher and/or weaker, and clouds encroach upon or envelop the summit. In fact, the unique terrain of Haleakala, with the summit sitting at the western end of a long, deep valley (the Haleakala caldera), can enhance convergence and sometimes force clouds up and over the summit even when the trade wind inversion is somewhat below the summit.

The objective of this work differs from previous efforts whose goals have been to characterize the atmospheric conditions with long-term measurement campaigns. In addition to building a database of standard atmospheric parameters, *in situ* data from a ground-based, infrared (IR), whole sky imager will be used, along with multispectral geostationary satellite imagery, atmospheric soundings and cloud forecasts from a numerical weather prediction model, and data from a ceilometer to characterize and predict cloud heights and cloud encroachment over the summit of Haleakala. This information will be used not only to quantify the effects of the atmosphere on FSOC communications and diagnose link disruptions, but also to develop atmospheric mitigation strategies that are essential to successful operations of future FSOC systems.

2. Technical Approach

In this study, *in situ* atmospheric measurements are being combined with remote sensing data and Numerical Weather Prediction (NWP) modeling to quantify the effects of the atmosphere on FSOC communications, to diagnose link disruptions, and to develop atmospheric mitigation strategies. The Weather Research and Forecasting (WRF) model is used to develop a climatology of OT over Haleakala, and this work examines aspects of the diurnal cycle of OT on Haleakala and its variations with terrain. In addition, WRF is used to generate a three-dimensional representation of C_n^2 and other atmospheric parameters in both the planetary boundary layer and the free atmosphere that can be used to help identify and forecast cloud blockages and poor seeing conditions.

This study also describes satellite products and plans for *in situ* instrumentation on Haleakala. This includes a description of high-resolution, satellite-derived cloud products, and how this data can be used for FSOC cloud mitigation. A description of a suite of ground-based sensors, including a meteorological station, a whole-sky imager, and a ceilometer that will be deployed on the summit of Haleakala is also provided. This is followed by a discussion of how these measurements will be combined with output from WRF to support mission planning and the development of operational concepts for mitigating link outages. This will include using vertical atmospheric soundings from the WRF model along with multispectral satellite imagery and ground-based cloud products to characterize and predict cloud heights and cloud encroachment over the summit of Haleakala. The following sections discuss WRF setup and products, satellite-derived cloud products, and plans for the *in situ* instrumentation on Haleakala.

a. WRF Model Setup and Products

The WRF model, developed jointly by the National Center for Atmospheric Research (NCAR) and the National Oceanic and Atmospheric Administration (NOAA) (Skamarock et al., 2008), is used in this study. WRF is a mesoscale NWP model developed for the prediction of weather and is routinely used by the National Weather Service and other forecasting services. The model is based on the Navier Stokes equations, which are solved numerically on a three-dimensional grid. The model simulates four basic atmospheric properties, wind, pressure, temperature, and atmospheric water vapor. All others variables are derived from these. The standard version of WRF does not produce optical turbulence parameters. However, in this application the model is modified to make simulations of C_n^2 based on changes to the Mellor-Yamada-Janjic (MYJ) TKE scheme to diagnose the turbulent Prandtl number as a function of the Richardson number (Alliss and Felton, 2009).

WRF is configured at 1-km horizontal resolution with dimensions of 272x272 grid points and 83 vertical levels. The resolution of the vertical levels is approximately 50-100 m below 2 km above ground level (AGL), 150-250 m for 2–13 km AGL, and 500 m up to the model top (50 millibars). Simulations are initialized at 1200 UTC directly from the 0.5° Global Forecasting System (GFS) analysis produced by the National Weather Service. Lateral boundary conditions are provided out to 27 hours by three-hourly GFS forecasts. This allows for filtering out model "spin-up" by excluding the first three simulation hours, while still capturing the full 24-hour diurnal cycle. The innermost of three nested WRF domains is shown in Figure 2.

The WRF output files contain time-varying, three-dimensional data, with values at each grid point representing standard meteorological quantities of temperature, pressure, winds, and moisture. Among many other optional parameters that can be specified, our modified WRF writes out the atmospheric refractive index structure

function, C_n^2. The seeing parameters of interest to astronomers and optical communications system designers can be derived from the refractive index structure function, C_n^2 (Andrews and Phillips, 2005). These products are used to generate vertical atmospheric soundings, similar to those obtained by radiosondes, above any location in the WRF domain. These soundings are used to identify and ultimately forecast the presence, strength, and height of trade wind inversions that indicate the likelihood of clouds obscuring the summit. An example of a WRF sounding is shown in Figure 3.

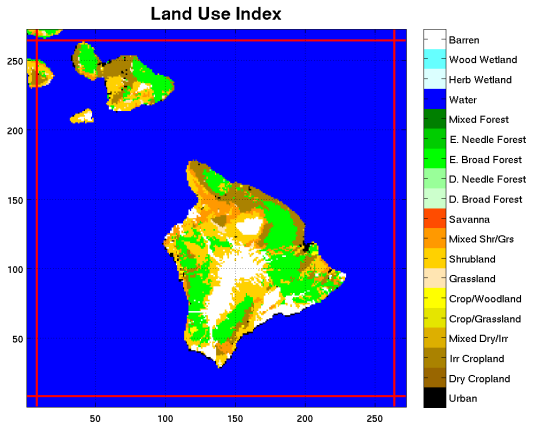

Figure 2 Land usage data for the innermost WRF domain. Land usage is critical in accurately describing optical turbulence.

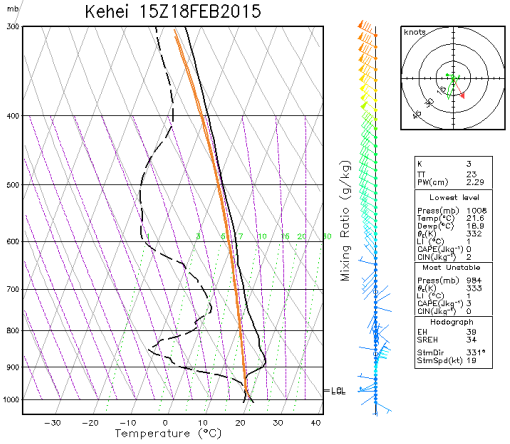

Figure 3 Example atmospheric vertical sounding from WRF. Temperature, dew point, and winds are shown on a Skew-T thermodynamic diagram.

c. Satellite Products

A main objective of this work is to detect and characterize clouds near and above the summit of Haleakala. One way to accomplish this is to use multispectral geostationary satellite imagery. Northrop Grumman has been collecting and processing multispectral satellite cloud imagery in support of FSOC mitigation studies for more than 18 years. For this investigation, the detection of clouds from satellite imagery is performed using the Cloud Mask Generator (CMG). The CMG ingests Geostationary Operational Environmental Satellite (GOES) multispectral imagery (at 4 km, 15 minute resolution) and applies a series of single- and multi-spectral tests to detect clouds (Alliss et al. 2000, Wojcik et.al., 2005). The GOES imager has 5 bands: visible (0.6 µm), shortwave infrared (3.9 µm) (SWIR), water vapor (6.7 µm), longwave infrared (10.7 µm) (LWIR), and split window (11.2 µm). The water vapor channel is not used for cloud detection and is replaced by a fog product at night and a shortwave reflectivity product during the day. The CMG generates a cloud/no cloud decision for every pixel by computing the difference between the LWIR temperature, visible albedo, derived products, and the dynamically computed clear sky background (CSB) each time a new GOES image is available. The classification of a pixel as clear or cloudy is based on where the calculated difference falls with respect to the threshold confidence range.

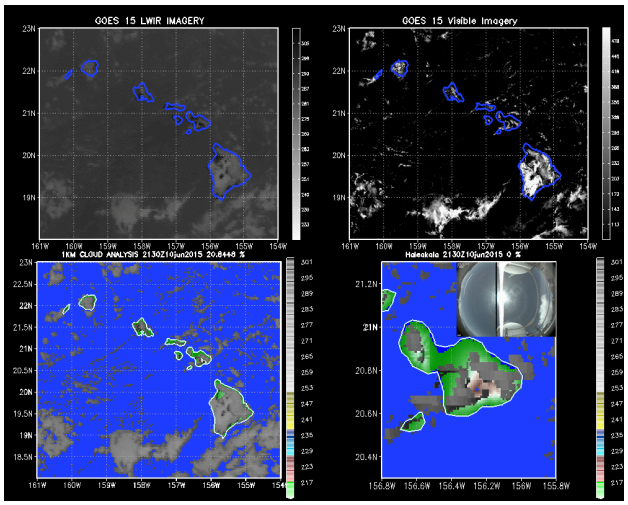

Figure 4 CMG example for Hawaii showing GOES LWIR (upper left) and GOES visible (upper right) images, the regional cloud mask shaded with the cloud top temperature (lower left), and the cloud mask for Maui (lower right). In addition, a whole sky imager located at the summit is also shown for comparison to the CMG.

Threshold confidence ranges for each test are spatially and temporally defined. The limit of the CMG cloud detection is estimated to be between 1.0 and 1.5 dB (Alliss et al. (2000)). A CMG example displaying the LWIR and visible imagery along with the CMG cloud mask for the Hawaii region is shown in Figure 4.

There are many benefits to geostationary satellite data that include its availability over most of the Earth as frequently as every 15 minutes. There are also limitations, and these can make cloud detection particularly difficult in the vicinity of isolated mountain tops with steep terrain such as the Haleakala summit. For an FSOC ground station on the relatively small summit of Haleakala, it is critical to determine whether clouds detected by the CMG above or in close proximity to the site will actually block the line-of-sight (LOS) to the communications satellite. Although the resolution of GOES imagery is as fine as 1-km in the daytime (visible channel only), clouds around the summit can be sub-grid scale and evolve rapidly. The GOES grid point that includes the peak of Haleakala (referred to hereafter as the Haleakala grid point) also includes some of the mountainside, and the terrain within the 4-km footprint ranges from about 2500 to 3055 meters AMSL. Even within the 1km GOES visible grid points, the terrain varies nearly 300 meters vertically. For this reason, the CMG sometimes legitimately identifies the Haleakala grid point as cloudy, when in fact *most* of it was cloudy, but only below 2800 meters AMSL. To minimize the impact of this type of error, the standard CMG algorithm is being supplemented with a cloud-top height (CTH) discriminator from surrounding grid points. Since the trade wind inversion keeps the cloud layer height relatively uniform and well-behaved around the mountain, the cloud-top temperature obtained from the GOES LWIR measurements from surrounding grid points can be used to refine the cloud decision for the summit. This is useful in identifying those times when the CMG identifies the Haleakala grid point as cloudy, but the cloud tops are actually a few hundred meters below the summit. The CTH is also valuable for forecasting whether clouds are likely to obscure the LOS in the near future. Examples of the use of GOES imagery, the CMG, and CTH are discussed in the results section.

c. Plans for in situ Instrumentation

Satellite imagery and WRF modeling are available for Haleakala now, but neither is sufficient to detect or forecast small-scale, dynamic clouds that can rapidly encroach upon the Haleakala summit and obscure the LOS between the ground station and a satellite. For example, sometimes most of the CMG grid point is clear, but a small cloud element exists within it that may block the LOS to a satellite. Additionally, these data are insufficient to diagnose transmission losses on the link during FSOC experiments. Therefore, the CMG products and WRF model output are being supplemented with *in situ* instrumentation that will monitor clouds, cloud attenuation, cloud heights, aerosols, and general weather conditions on Haleakala in an effort to characterize the long-term climatology of clouds and other atmospherics at the site. The data will also serve to validate the satellite-based cloud climatology (CMG) as well as be used to develop methods and standards for future atmospheric characterization and forecasting requirements. The equipment includes an infrared whole sky imager (WSI) that can detect and characterize clouds at high spatial and temporal resolution both day and night. The WSI will be supplemented by a cloud lidar (ceilometer) that will measure the cloud heights, physical thickness, and cloud fade (dB). The ceilometer data may also be useful in identifying aerosols and the inversion height in some cases. In addition to identifying the presence of clouds, the output of the WSI and ceilometer will be used for link diagnostics such as explaining transmission losses on a space-to-ground link. Finally, a standard meteorological station will measure and archive temperature, pressure, humidity, and winds that are useful in overall site characterization and mission management requirements.

3. Results

The characterization and modeling of atmospheric conditions pertaining to FSOC operations includes several facets. As previously discussed, the success of FSOC systems depends on the successful mitigation of atmospheric effects, primarily cloud cover and optical turbulence. This section discusses the measurement and modeling of atmospheric effects in support of using Haleakala as a laser communications ground station. First, turbulence statistics for Haleakala generated from WRF modeling are presented. Second, cloud statistics of Haleakala obtained from the CMG are discussed along with an analysis of the trade wind inversion height and its impacts on clouds. Next, two case studies are presented that demonstrate the importance and difficulty of cloud forecasting on the summit of Haleakala. Finally, FSOC mission planning and atmospheric mitigation strategies for a ground station on Haleakala are discussed.

a. Haleakala Optical Turbulence

WRF is used to make three-dimensional turbulence simulations over the state of Hawaii once per day during a nearly two-year period. A modified version of WRF that computes the atmospheric refractive index structure function, C_n^2, for every three-dimensional grid point in the WRF domain is employed. From this data, profiles of C_n^2 can be extracted for any line-of-sight within the domain. C_n^2 is integrated vertically to compute the Fried coherence length, r_0, which is a measure of phase distortion of an optical wave front by turbulence. This parameter represents the integrated effect of turbulence along a line of sight, and can vary rapidly over time and from one point of the sky to another. Larger values of r_0 are indicative of less turbulence and better seeing, while smaller values of r_0 represent stronger turbulence and worse seeing. The coherence length (Fried, 1965) is calculated by integrating C_n^2 along a path, z:

$$r_o = \left[0.423 \left(\frac{2\pi}{\lambda} \right)^2 \int_0^\infty C_n^2(z)\, dz \right]^{-3/5}$$

The cumulative distributions of r_0 derived from the WRF simulations for the AMOS site on Haleakala are shown in Figure 5. The values shown only represent the times when WRF shows the site to be cloud-free, *i.e.* times where the total cloud liquid water and ice water content are very near zero. Haleakala exhibits a significant difference between the values of r_0 during the daytime and those simulated during the nighttime hours. The plot shows the median overall value of r_0 is 10.9 cm, while the daytime and nighttime median values are 9.3 cm and 13.1 cm, respectively. These values are consistent with those reported by Bradley et. al 2006, which gives median day and night values of r_0 of 9.7 cm and 14.7 cm, respectively. Differences are likely explained by local effects such as differential heating and disruptions in wind flow due to terrain features and man-made structures that occur on a smaller scale than can be modeled by WRF.

A diurnal cycle in r_0 is expected for most locations over land, since daytime heating of the land creates thermal instability and drives the creation and maintenance of strong atmospheric turbulence. At night the land cools, the lower atmosphere becomes thermally stable, and turbulence is suppressed. The degree to which this happens and the relative strengths of daytime and nighttime turbulence vary by location, governed by phenomena such as surface heat capacity, elevated nocturnal temperature inversions, and wind speed.

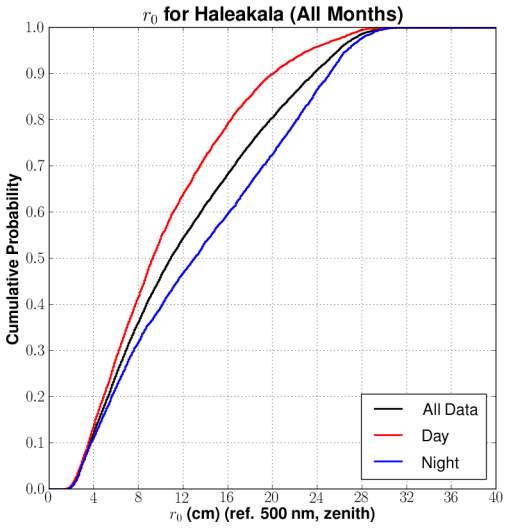

Figure 5 Cumulative distributions of r_0 for Haleakala for all times (black), day (red), and night (blue). Values of r_0 are referenced to 500 nm and zenith.

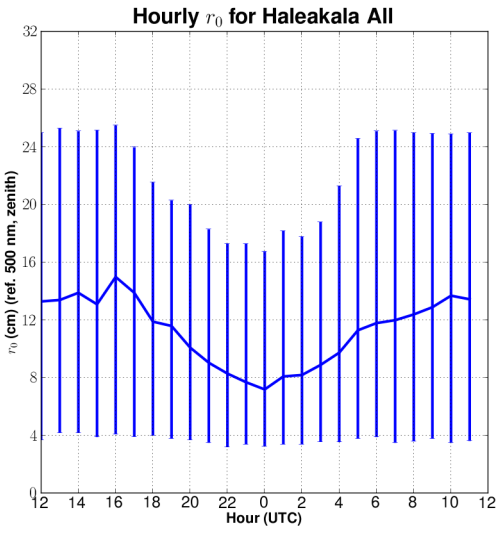

Figure 6 Median hourly r_0 at Haleakala with the 5% and 95% data intervals shown by the vertical bars.

A diurnal variation of r_0 at Haleakala is clearly observed in Figure 6. In this plot, the line that connects the vertical bars shows the median value of r_0 for each hour of the day. The vertical bars show the range of 90% of the data for each hour, from the 5% value at the bottom to the 95% value at the top of each bar. The values of r_0 decrease after sunrise (~1700 UTC, 7 AM local), reach their minimum near and just after local noon (2200-0200 UTC), and rise in the late afternoon maintaining large values throughout the night. The data indicate r_0 varies between about 3.5 cm and 17 cm during mid-day and early afternoon hours when the surface heating is at its maximum. The seeing is much better during the nighttime hours, but the 5% values show there are times where the seeing is quite poor at night. This generally occurs when winds are stronger, as indicated in the two-dimensional histogram of r_0 and wind speed shown in Figure 7. This plot shows the nighttime r_0 value is usually less than 6 cm when the wind speed is greater than 6 m/s (approximately 12 kts). When the distributions of r_0 are separated by the concurrent wind speeds (Figure 8) it becomes evident that atmospheric seeing is usually quite poor when winds are greater than 15-20 kts on the summit of Haleakala. This is consistent with observations from Bradley et al. 2006 that show a correlation of r_0 with wind speed. Their data from the Day Night Seeing Monitor (DNSM) on Haleakala show degradation in seeing with increased wind speeds. They also report a dependence of r_0 with wind direction at the summit of Haleakala that is also evident in the WRF data shown by the distributions of r_0 with direction in Figure 9. With prevailing winds from the northeast to east (60°-90°), the air must cross over the Haleakala caldera before reaching the observatories on Haleakala. This has the effect of increasing the turbulence immediately above the site, and is more prevalent during the night than day.

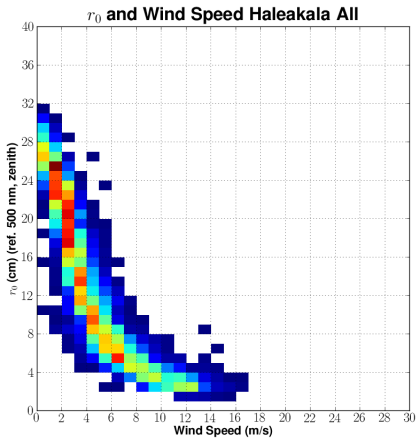

Figure 7 Two-dimensional histogram showing the frequency of occurrence of r_0 and wind speed.

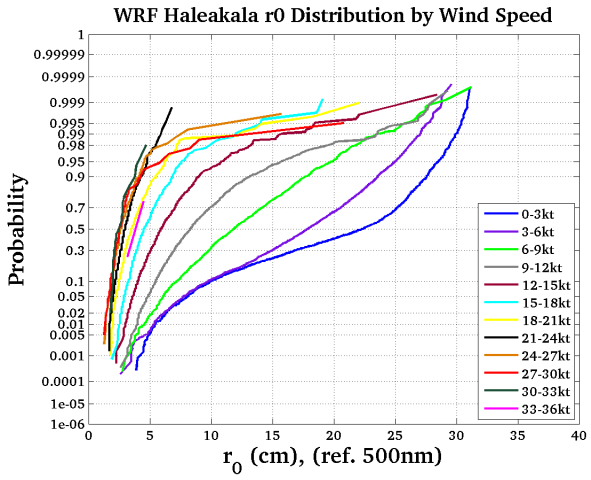

Figure 8 Distributions of r_0 for multiple ranges of wind speeds. Optical turbulence is more severe when winds are strong.

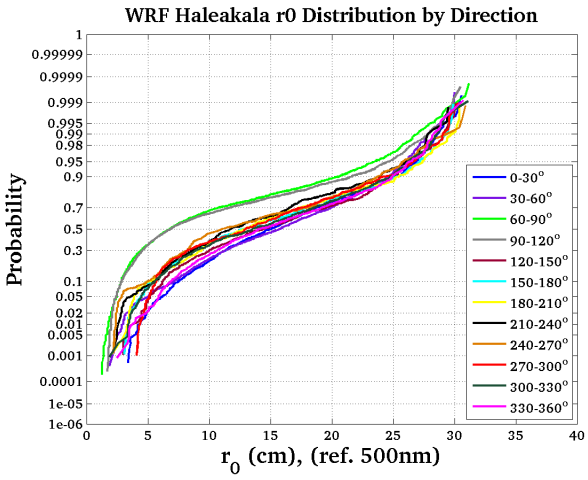

Figure 9 Distributions of r_0 for multiple ranges of wind directions. Optical turbulence is more severe when winds blow from the east or northeast.

b. Hawaii Inversion Statistics

As introduced earlier, the trade wind inversion is a common feature in Hawaii, and is a dominant factor in whether convective clouds grow to heights at which they might block an optical link from a satellite to a ground site

on the summit of Haleakala. When a strong inversion is present, as indicated by an increase in temperature with height and a discontinuity in atmospheric moisture, it limits the height to which clouds can grow. This is supported by cloud statistics derived from the CMG analysis, which indicate the summit of Haleakala is cloud-free approximately 70% of the time, while the surrounding slopes just below the summit are cloud-free only about 58% of the time. A good example of this is shown by the 2000 UTC GOES imagery and CMG cloud mask from July 31, 2015, in Figure 10 and the 1200 UTC radiosonde data from Hilo, HI, on the same day in Figure 11. The increase in temperature shown by the solid black line in Figure 11 near 770 mb (about 2400 m AMSL) along with the sharp decrease in the dew point temperature represented by the dashed black line clearly indicate the presence of a trade wind inversion. The temperature increases from 12.8 °C to 14.6 °C and the dew point temperature decreases from -0.2 °C to as low as -10.0 °C between 2325 m and 2439 m AMSL. Since the summit of Haleakala is approximately 3055 m AMSL, the cloud layer is expected to be about 600 meters (nearly 2000 feet) below the summit on this day. This is indeed the case, with the GOES imagery and CMG analysis showing clouds only on the slopes of Haleakala. Further validation is provided by the WSI in Figure 10, which shows only clear skies at the summit. Conversely, clouds are likely to obscure laser communications to and from the summit when the trade wind inversion is weak or occurs at or above 3000 meters AMSL.

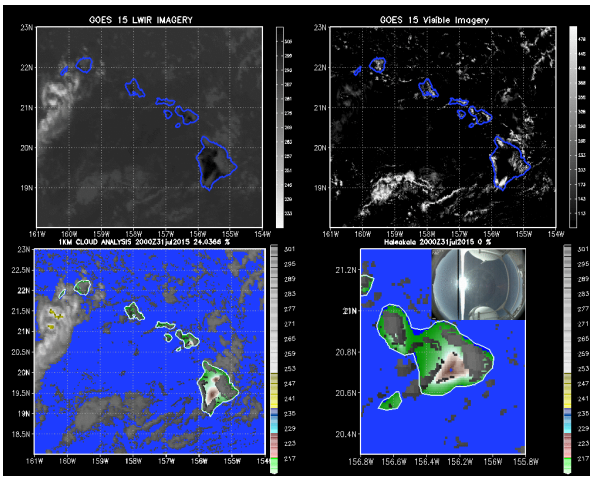

Figure 10 Example GOES imagery and resulting CMG cloud mask for 2000 UTC on July 31, 2015. WSI located at summit of Haleakala shows cloud-free conditions.

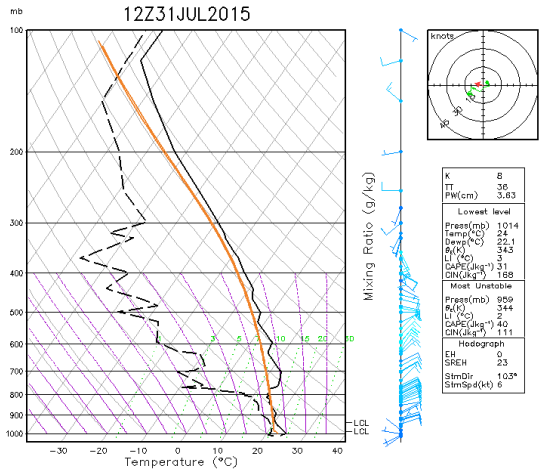

Figure 11 Skew-T Log-P diagram for Hilo, HI, for 1200 UTC on July 31, 2015. The inversion at this time is below the summit of Haleakala.

To determine the likelihood of low-level clouds interrupting FSOC communications on Haleakala, soundings from Hilo, HI, and Lihue, HI, are used to identify the trade wind inversion height. This is accomplished by using the vertical profiles of temperature and dew point temperature from each site to determine whether there is a strong inversion in each sounding. This was initially done with a well-established algorithm called the Heffter Planetary Boundary Layer (PBL) height method (Heffter, 1980). Using this algorithm, temperature inversions are determined from gradients in the potential temperature, and are identified as layers over which the potential temperature lapse rate is greater than 0.005 K/m. The PBL height, also the trade wind inversion height in Hawaii, is identified as the lowest of these inversion layers over which the increase in potential temperature is larger than 2 K. In the example shown in Figure 11, the potential temperature gradient is 0.034 K/m and the increase in potential temperature is 3.5 K, indicating a relatively strong, easily identifiable trade wind inversion is present. However, visual comparisons of the results with Skew-T Log-P diagrams from Hilo reveal the Heffter algorithm often identifies multiple inversions, many of which are not accompanied by a significant decrease in humidity. This makes it difficult to automatically distinguish the true trade wind inversion with an algorithm based only on the temperature gradients.

Since the trade wind inversion in Hawaii is marked by both an increase in temperature and a sharp decrease in atmospheric moisture with height, the Heffter algorithm is supplemented in this study with a dew point depression test, where the dew point depression is the difference between the temperature and dew point temperature. Results show the trade wind inversion can be identified as the lowest layer above the lifting condensation level (LCL) meeting the Heffter thresholds and having a dew point depression greater than 7 K. Heights of the inversions are accumulated in order to find the median inversion height, as well as the probability that the inversion height is above

3000 m. The data in Figure 12 show the vertical profiles of the medians of several parameters from the 0000 UTC (1400 HST, daytime) Hilo (PHTO) radiosonde data. The dark blue and red lines show the temperature and dew point temperature profiles, respectively, while the cyan line displays the dew point depression. The horizontal dashed purple line is plotted at the height of the median LCL, and the horizontal dashed orange line shows the median height of the trade wind inversion, and is indicative of the cloud top height of interest to FSOC. This data shows the median inversion height is about 2225 meters (7300 feet) AMSL, and is coincident with a distinctive increase in the median dew point depression at that level. The cumulative distributions of the heights of the Hilo LCL and trade wind inversion are shown in Figure 13. This data indicates the trade wind inversion, when present, exists below the summit of Haleakala (3055 meters AMSL) approximately 86% of the time. The inversion analysis also shows seasonal differences in the trade wind inversion height as displayed in Table 1.

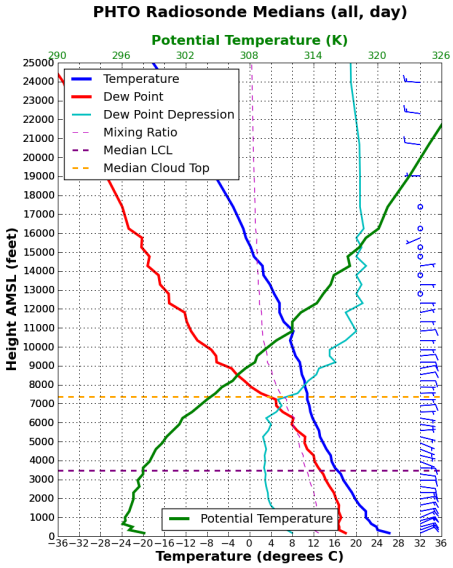

Figure 12 Median profiles of temperature (dark blue), dew point temperature (red), dew point depression (cyan), mixing ratio (dashed lavender), and potential temperature (green) from Hilo, HI, radiosonde data.

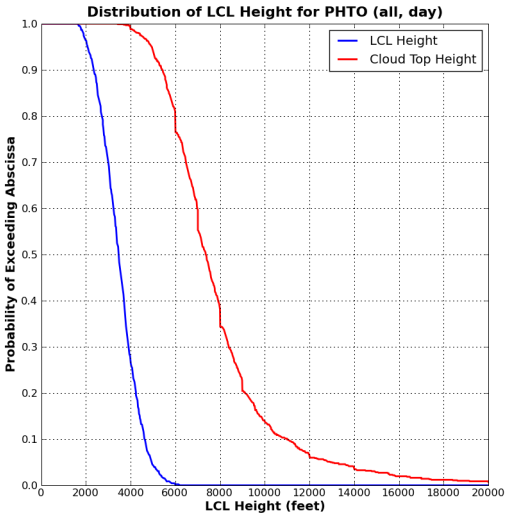

Figure 13 Cumulative distributions of the heights of the LCL (blue) and trade wind inversion (red) for Hilo, HI.

Table 1 Median height (meters AMSL) of the daytime trade wind inversion for Hilo and Lihue, HI, by season.

	Spring (MAM)	Summer (JJA)	Fall (SON)	Winter (DJF)
Hilo	2400	2225	2150	2150
Lihue	2100	2050	2100	2000

This analysis has implications for the ability to accurately detect cloud encroachment on a future FSOC ground station on Haleakala. The data show the trade wind inversion usually keeps clouds below the summit. However, the radiosonde data from Hilo shows the inversion sometimes exists at or above 3055 meters, and clouds are likely to rise above the summit on these days. In fact, the unique topography of Haleakala, with the summit sitting at the western end of the Haleakala caldera, can sometimes force clouds up and over the summit even when the trade wind inversion is somewhat below the summit. This analysis indicates cloud encroachment on the summit could present problems to FSOC about 15-20% of the time when the trade wind inversion is present. The strength and height of the trade wind inversion may also be dependent upon the wind direction. CMG results show a dependence of the occurrence of clouds with wind direction (Figure 14). Clouds are less likely to obscure the summit of Haleakala when the wind is blowing from the east or northeast, *i.e.* when the trade wind inversion is most likely to be present. Clouds are most likely to obscure the summit when winds blow from the south. This perhaps indicates a relationship between the wind direction, the inversion height, and the presence of clouds on the summit of Haleakala. Further research is required to address this, and the results will be improved with high-resolution data from the ground-based WSI.

c. Case Studies

To illustrate the benefits and difficulties of using the Hilo radiosonde data as an indicator or predictor of cloud obscuration on the summit of Haleakala, soundings from two days in June 2015 are shown. These two days are typical, and exemplify different atmospheric conditions and their impacts on the short-term prediction of cloud outages on Haleakala. The Hilo sounding from 0000 UTC on June 21, 2015, shows a strong trade wind inversion near 770 mb. Displayed in the right panel of Figure 15, the inversion near 2400 meters (7871 feet) AMSL is characterized by a potential temperature gradient of 0.028 K/m, an increase in potential temperature of 3.1 K, and a corresponding decrease in dew point temperature of over 20 K. The GOES visible satellite imagery in the upper middle panel of Figure 15 shows clouds (denoted by white shades) on the slopes of Haleakala, with the upper reaches of the mountain being cloud-free (cloud-free areas shown in black). This is also evident in the LWIR imagery which shows cloud top temperatures and skin temperatures of the surface where it is clear (upper left panel), and the CMG uses this data to correctly identify the clouds in and around Maui (lower left panel) with cloud tops indicated to be between 2000 and 2500 meters AMSL. The lower middle panel shows the cloud base heights from the Kahului (PHOG) airport. At the time of the GOES image, 2145 UTC, there are two cloud layers identified at Kahului – one with the cloud base height at about 500 meters and the second near 1500 meters AMSL. This is consistent with the data from the sounding and the GOES imagery, which shows its cloud heights are less than 3055meters.

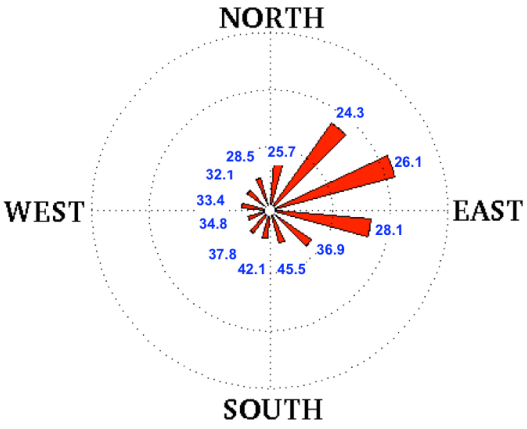

Figure 14 Wind rose plot showing the frequency of occurrence of clouds (blue numbers, percentage) on the summit of Haleakala according to the CMG by wind direction. Clouds are less likely when the trade winds are blowing (easterly and northeasterly winds).

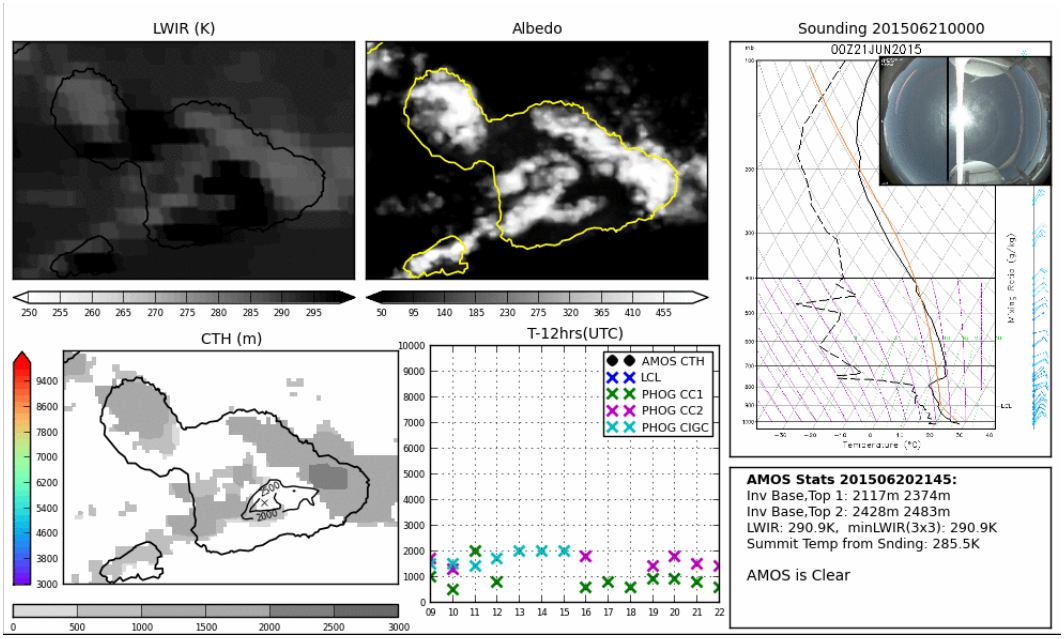

Figure 15 GOES LWIR temperatures (upper left) and visible (upper middle) imagery with the CMG cloud top heights (lower left) and recent cloud layer information (lower middle) for 2145 UTC June 20, 2015. The Hilo radiosonde from 0000 UTC June 21, 2015 is shown in the right panel with an overlay of the WSI image from the Haleakala summit showing clear skies.

Given the relatively coarse resolution of the GOES data and the fact that the Hilo sounding is more than 160 km from Haleakala, WRF was used to model the atmospheric conditions over Hawaii on June 20, 2015. For this task, WRF 3.6.1 was set up to run three domains over a region containing Hawaii with horizontal resolutions of 16, 4, and 1-km and 81 vertical levels from the surface up to 50 mb. The WRF run was initialized from the 0.5 degree GFS data at 0000 UTC on June 20, 2015. Output from WRF in Figure 16 for the same time shows conditions similar to those observed in the Hilo sounding, with a temperature inversion near 750 mb and a corresponding sharp decrease in humidity. The clouds predicted by WRF (Figure 16b) are also similar in coverage and heights to those identified by the CMG cloud mask.

In contrast with June 20, the mid-day atmosphere on June 10 does not have a strong trade wind inversion below the summit of Haleakala. As a result, clouds grow to levels that can cause outages for an optical link to a ground station on Haleakala. The sounding from 0000 UTC on June 11, 2015, in the right panel of Figure 17 shows a weak inversion near 750 mb (about 2600 meters AMSL). The potential temperature gradient is 0.019 K/m, but the total increase in potential temperature over the layer is only 1.3 K, and does not meet the criteria for a Heffter inversion. The actual trade wind inversion on this day is located well above the summit near 630 mb or about 4000 meters AMSL. The dew point profile shows a dry layer near 2600 m, but also a layer with higher humidity near the trade wind inversion at 3700 m that may be conducive to cloud formation. Similar to the Hilo radiosonde data, no trade wind inversion exists below the Haleakala summit in the WRF sounding shown in Figure 18a for this day. This allows clouds to form and extend to the upper reaches of the mountain in the WRF simulation, and the WRF output (Figure 18b) shows a cloud field quite similar to the GOES visible imagery (Figure 17) over Maui. In fact, WRF predicts clouds to grow to more than 3800 meters on the Big Island of Hawaii, evidenced by their obscuration of all but the summits of Mauna Loa and Mauna Kea at more than 4000 meters AMSL.

The GOES satellite imagery does indeed show cloud formation higher up the mountain on this day and the summit intermittently obscured by clouds. This is supported by the clouds visible in the picture from whole sky imager in the upper right panel of Figure 17. Although not overcast, the WSI image shows the small, dynamic cloud elements that form and move above the summit of Haleakala when the trade wind inversion is weak, above the summit, or absent. These clouds, often considerable smaller than even the 1-km resolution of the GOES visible imagery, are difficult to detect from geostationary satellite data. In addition, they can evolve quite rapidly, changing size and shape and moving through the LOS over the course of seconds and minutes – faster than the 15 minute time resolution of the GOES imagery. The apparent horizontal coverage of clouds appears to be quite similar in the vicinity of Haleakala when comparing the visible imagery for the two cases (GOES visible images in Figure 15 and Figure 17). This is misleading, however, due to the severe slope of the terrain near the summit, and makes precise cloud characterization using GOES very challenging. For these reasons, existing meteorological data, i.e. satellite imagery and radiosonde data, must be supplemented with *in situ* data measured at the site itself.

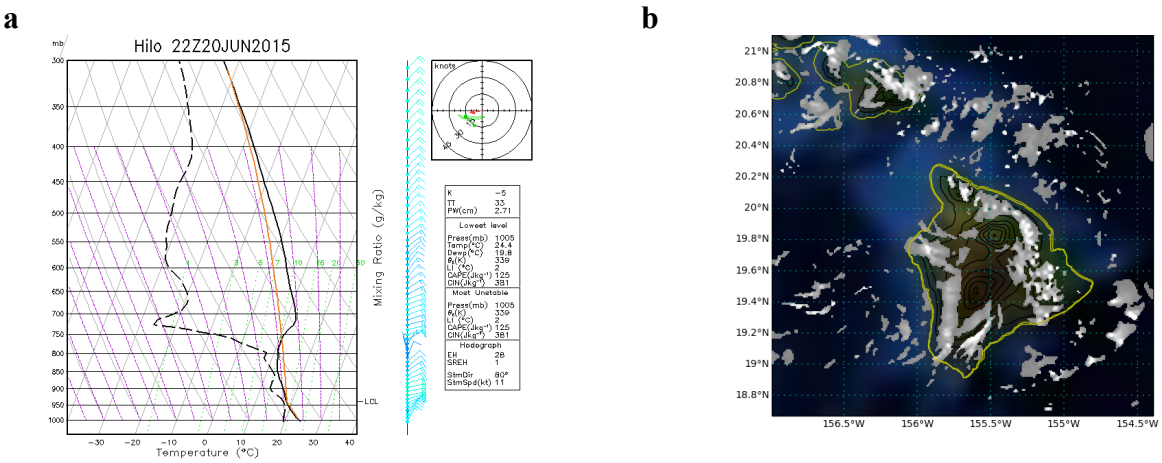

Figure 16 (a) Skew-T Log-P diagram from WRF forecast for 2200 UTC on June 20, 2015 with temperature (solid black line) and dew point temperature (dashed black line). (b) Clouds predicted by WRF at 2200 UTC on June 20, 2015.

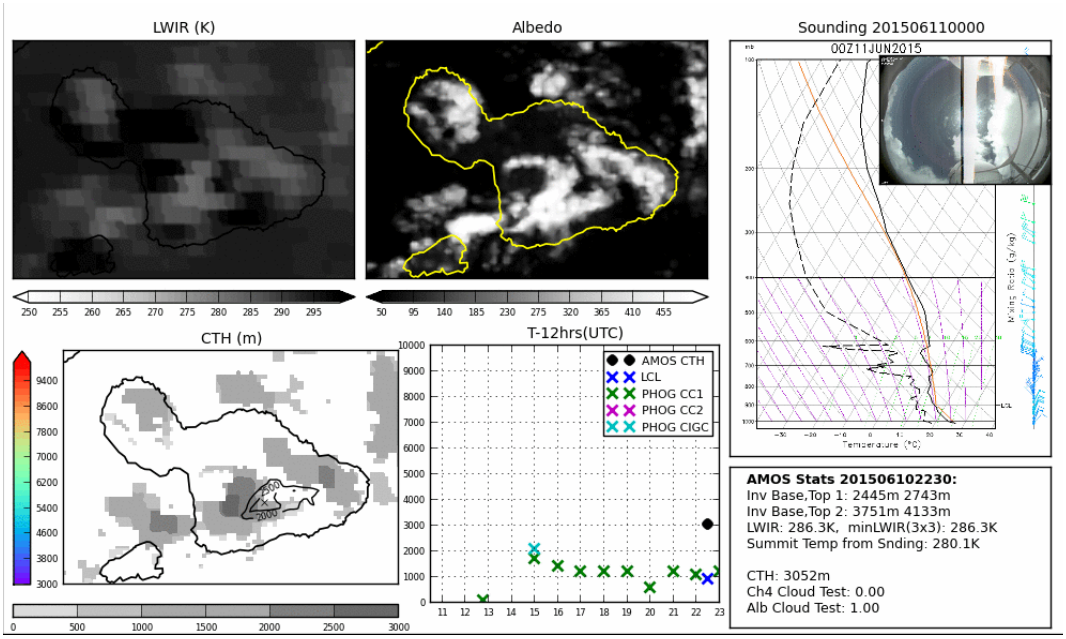

Figure 17 GOES LWIR (upper left) and visible (upper middle) imagery with the CMG cloud mask (lower left) and recent cloud layer information (lower middle) for 2230 UTC June 10, 2015. The Hilo radiosonde from 0000 UTC June 11, 2015 is shown in the right panel with an overlay of the WSI image from the Haleakala summit.

a **b**

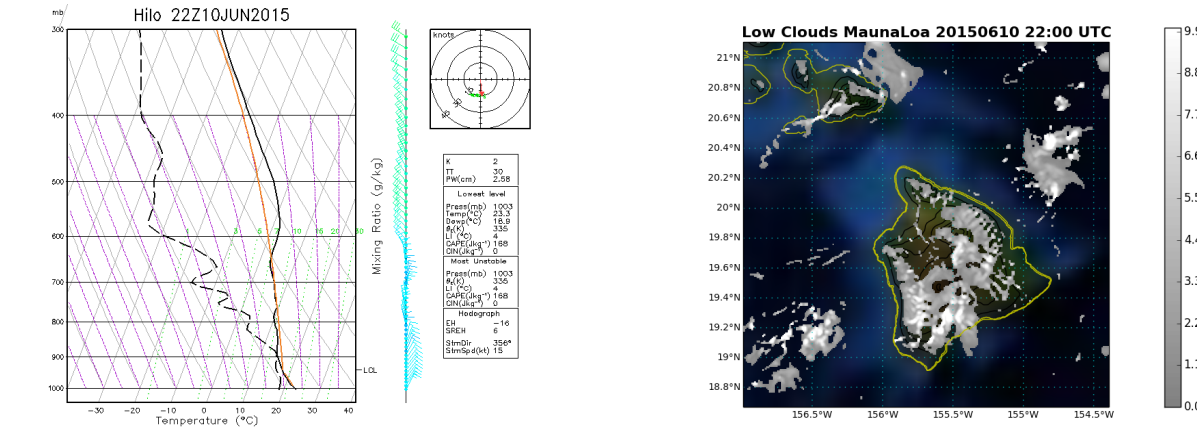

Figure 18 (a) Skew-T Log-P diagram from WRF forecast for 2200 UTC on June 10, 2015 with temperature (solid black line) and dew point temperature (dashed black line). (b) Clouds predicted by WRF at 2200 UTC on June 10, 2015.

d. Mission Planning and Mitigation Strategies

Whatever the mission, characterizing and predicting atmospheric conditions, especially cloud attenuation, is critical to the success of FSOC systems. Thus far, some of the capabilities and limitations of currently available meteorological data, satellite products, and NWP modeling techniques have been discussed. While valuable to many aspects of FSOC operations, this data lacks the resolution to detect or forecast small-scale, dynamic clouds that can rapidly encroach upon the Haleakala summit and obscure the LOS between the ground station and a satellite. Additionally, these data are insufficient to diagnose transmission losses on the link during FSOC

experiments. To mitigate these risks, supplemental instrumentation is being considered for Haleakala. This *in situ* instrumentation will monitor clouds, cloud attenuation, cloud heights, aerosols, and general weather conditions in an effort to characterize the long-term climatology of clouds and other atmospherics at the site. The data will also serve as ground-truth to validate the long-term CMG statistics and quantify what biases, if any, exist in the satellite-derived cloud products for Haleakala. All of these sources of information will be analyzed and combined to develop methods and standards for future atmospheric characterization and forecasting requirements.

Perhaps the most important instrument that will be deployed is an infrared whole sky imager that will provide radiometrically-calibrated imagery in the mid-infrared (mid-IR). The mid-IR WSI provides imagery both day and night at high spatial and temporal resolution, enabling the detection of small, rapidly evolving clouds that may not be detectable from the GOES imagery. This is particularly important at Haleakala since clouds are often present just below the site and can rapidly encroach upon the site with slight changes in the planetary boundary layer structure or atmospheric dynamics. A ceilometer is also planned to determine the cloud heights and cloud attenuation. The ceilometer uses a laser to send a pulse with a duration on the order of nanoseconds through the atmosphere. Some of the light is scattered by cloud droplets and aerosols and a small fraction of this is directed back to the receiver. In addition to cloud heights and physical depths, estimates of the cloud fading and boundary layer height can be computed from this information. Finally, a meteorological station will collect and archive standard meteorological data to include wind speed and direction, temperature, pressure, and humidity.

Although some atmospheric degradations and outages will be unavoidable for an operational FSOC system, many of the impacts of the atmosphere can be reduced or eliminated with accurate atmospheric characterization and modeling. Each of the tools, products, and techniques described in this paper are designed to address one or more components in the development of an effective strategy to mitigate atmospheric losses and maximize data throughput on FSOC systems. Atmospheric mitigation strategies should be tailored to specific mission concepts of operations (CONOPS). For example, if a satellite has large amounts of onboard storage and high data rates and latency is not a concern, it might be possible to wait and retransmit the data when the LOS becomes cloud-free. However, if latency is important, multiple, diverse ground stations are required to increase the probability of at least one having a cloud-free line of sight (CFLOS). Different missions may require different forecast lead-times. Some CONOPS, perhaps a deep-space probe, may require several hours' notice of poor conditions. Near-Earth missions may also desire forecasts out to several hours, but have a critical need of precise forecasting only out to a few minutes.

An atmospheric mitigation strategy is envisioned that takes into account mission CONOPS, and applies the available information at the appropriate time scales. NWP modeling provides a forecast of weather conditions from a few hours to a few days in the future. The high-resolution version of WRF provides additional information on the temperature structure, clouds, and turbulence in the vicinity of Haleakala. The second time scale is for forecasts of minutes to a few hours. Predictions for this time period will be derived from the CMG and from the characteristics of the trade wind inversion derived from radiosonde data. Data from the CMG indicate where the clouds are located currently, as well as provide an estimate of the cloud top height (CTH). Clouds are usually present over and around Hawaii, but often exist only in the lowest few thousand meters of the atmosphere. The CTH is useful to determine whether clouds located in the vicinity of the LOS between Haleakala and a satellite are actually high enough in the atmosphere to block the link, preventing over-prediction of cloud impacts from satellite imagery. In addition, the CMG data may be used to provide a persistence forecast based on the consistency of recent conditions. As discussed previously, the height and strength of the trade wind inversion is indicative of the likelihood that clouds will rise above the altitude of the Haleakala summit. The WSI imagery will be used to identify small, rapidly evolving clouds that may be a danger to the FSOC transmission in the next few seconds or minutes. Cloud characteristics from the ceilometer, including cloud height and optical channel fading, will be used to validate the CMG data and to diagnose link outages. Finally, FSOC ground station operations can be affected by ambient weather conditions, and a strategy must be in place to handle cases of high winds, precipitation, and condensation. The meteorological station on the site will provide realtime measurements of these parameters, and WRF will provide forecast of winds, precipitation, and clouds with a lead-time of a few hours to a few days.

Combined, this information will provide advance notice of potential link degradations and outages. This will trigger appropriate actions in the operations of the FSOC system based on the likelihood and severity of the atmospheric degradation as well as how soon it will impact the system. The response based on the mitigation strategy for an FSOC system may include any or all of a range of options such as switching the link to an alternate ground station, buffering the data for later transmission, reducing the data rate, or occasionally accepting the loss of data.

4. Summary and Conclusions

Optical communications provide a solution to the ever-increasing data needs of modern society. However, the ultimate realization of practical, high-availability FSOC systems will depend upon how well they mitigate the impacts of atmospheric effects. In support of this, Northrop Grumman is leading a campaign to measure and model the atmospheric effects on the link between a ground station on the summit of Haleakala and a satellite in geostationary orbit. In this study, plans to combine *in situ* atmospheric measurements with remote sensing data and NWP modeling to quantify the effects of the atmosphere on FSOC communications, to diagnose link disruptions, and to develop atmospheric mitigation strategies are discussed. To date, optical turbulence statistics have been generated for the Hawaiian Islands using a modified version of the WRF numerical weather prediction model. Results show WRF is able to produce realistic diurnal variations of optical turbulence as represented by the Fried coherence length, r_0. In addition, analysis of the trade wind inversion height is being used as a predictor of the probability of low-level clouds over the Haleakala summit. Initial studies show a correlation of the trade wind inversion strength and height with the presence of clouds on Haleakala. Case studies show some of the capabilities and limitations of currently available meteorological data, satellite products, and NWP modeling techniques with regards to identifying and predicting cloud outages at Haleakala. In particular, none of these existing technologies is sufficient to detect or forecast small-scale, dynamic clouds that can rapidly encroach upon the Haleakala summit and obscure the LOS between the ground station and a satellite. Therefore, the satellite-derived CMG products and WRF model output will be supplemented with *in situ* instrumentation that will monitor clouds, cloud attenuation, cloud heights, aerosols, and general weather conditions at Haleakala. Using this information, it is possible to not only quantify the effects of the atmosphere on FSOC communications and diagnose link disruptions, but also develop atmospheric mitigation strategies that are essential to successful operations of future FSOC systems.

References

Alliss, R.J., M. E. Loftus, D. Apling, and J. Lefever, "The Development of Cloud Retrieval Algorithms Applied to GOES Digital Data," in *10th Conference on Satellite Meteorology and Oceanography*, pp. 330–333, American Meteorological Soc., January 2000.

Alliss, R.J and B.D. Felton, 2009: "Validation of Optical Turbulence Simulations from a Numerical Weather Prediction Model in Support of Adaptive Optics Design", *Advance Maui Optical and Space Surveillance Technologies Conference*, Vol 1, p. 54.

Andrews, L.C. and R. L. Phillips, "Laser Beam Propagation through Random Media", second edition, SPIE press, 2005.

Bradley, E.S., L.C. Roberts, L. W. Bradford, M. Skinner, D.A. Nahrstedt, M.F. Waterson and J.R. Kuhn, 2006: Characterization of Meteorological and Seeing Conditions at Haleakala. *Publications of the Astronomical Soc. of the Pacific*, **118:**172-182.

Fried, D. L., 1965: Statistics of a geometric representation of wavefront distortion. *J. Opt. Soc. Amer.*, **55**, 1427–1435.

Haleakala Observatories, Institute for Astronomy, University of Hawaii, 2015: http://www.ifa.hawaii.edu/haleakalanew/observatories.shtml.

Heffter JL. 1980. "Transport Layer Depth Calculations." Second Joint Conference on Applications of Air Pollution Meteorology, New Orleans, Louisiana.

Mellor, G. L., and T. Yamada, 1982: Development of a turbulence closure model for geophysical fluid problems. *Rev. Geophys. Space Phys.*, **20**, 851–875.

Skamarock, W. C., J. B. Klemp, J. Dudhia, D. O. Gill, D. M. Barker, M. G. Duda, X.-Y. Huang, W. Wang, and J. G. Powers, 2008: A description of the advanced research WRF version 3. NCAR Technical Note, NCAR/TN-475+STR, 113 pp.

Wojcik, G., R.J., Alliss and M.E., Craddock, "Deep Space to Ground Laser Communications in a Cloudy World", *IEEE Photonics*, Aug 2005.